Supporting Information for

Watching lanthanide nanoparticles one at a time: characterization of their photoluminescence dynamics at the single nanoparticle level

Malavika Kayyil Veedu,[1] Gemma Lavilley,[2,3] Mohamadou Sy,[2] Joan Goetz,[2] Loïc J. Charbonnière,[3] Jérôme Wenger[1,*]

[1] *Aix Marseille Univ, CNRS, Centrale Med, Institut Fresnel, AMUTech, 13013 Marseille, France*

[2] *Poly-Dtech, 204 avenue de Colmar, 67100 Strasbourg, France*

[3] *Equipe de Synthèse Pour l'Analyse, Institut Pluridisciplinaire Hubert Curien (IPHC), UMR 7178 CNRS/University of Strasbourg, Cedex 2, 67087 Strasbourg, France*

** Corresponding author: jerome.wenger@fresnel.fr*

Contents:

S1. Background intensity after time gating

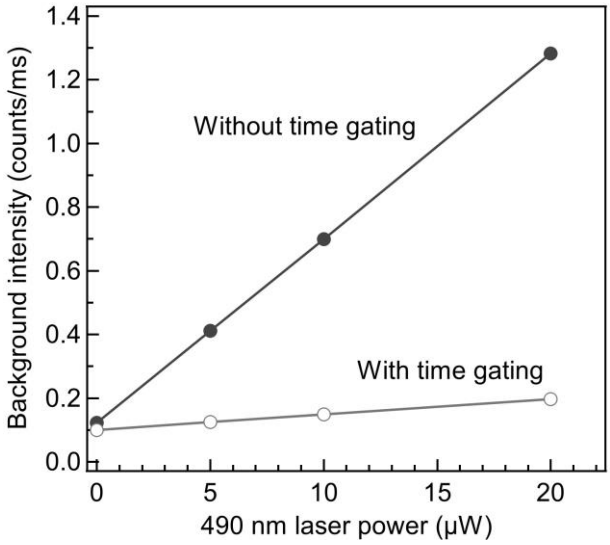

Figure S1. Evolution of the total background intensity recorded on a water solution without the LnNPs as a function of the 490 nm laser power. Filled markers indicate the experiment where all photons are counted, without applying any temporal gating. Empty markers show the background intensity reduction after applying a temporal gating filter where all photons incoming within the 0-3 ns interval are discarded for the analysis, as illustrated on the TCSPC data in Fig. 3a. Lines are linear fits to the data.

S2. Supplementary correlation data for SmNPs and EuNPs at different excitation powers

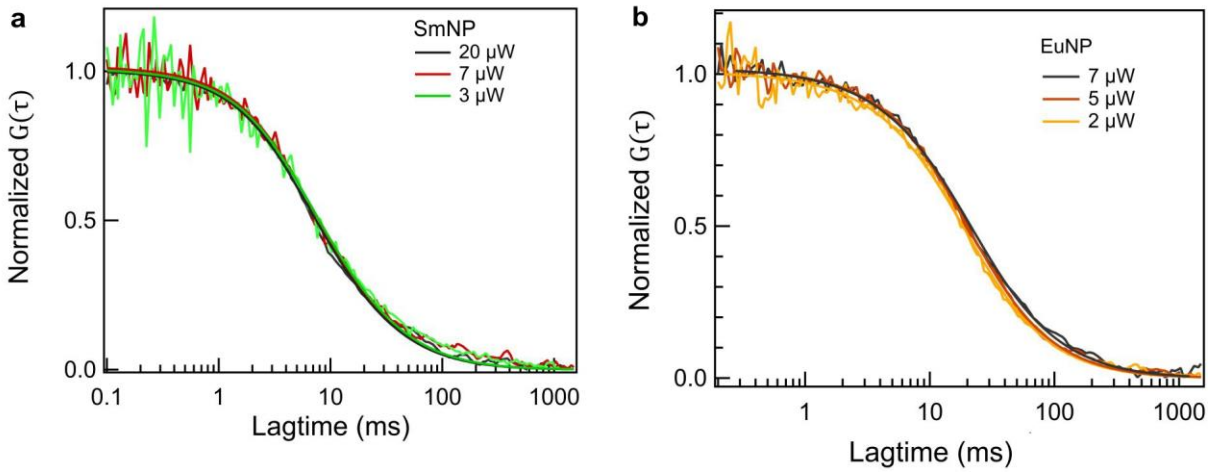

Figure S2. FCS correlation data for SmNPs (a) and EuNPs (b) at increasing excitation powers show a remarkable consistency in the correlation shape indicating no sign for blinking nor photobleaching.

S3. Fit residuals for different models

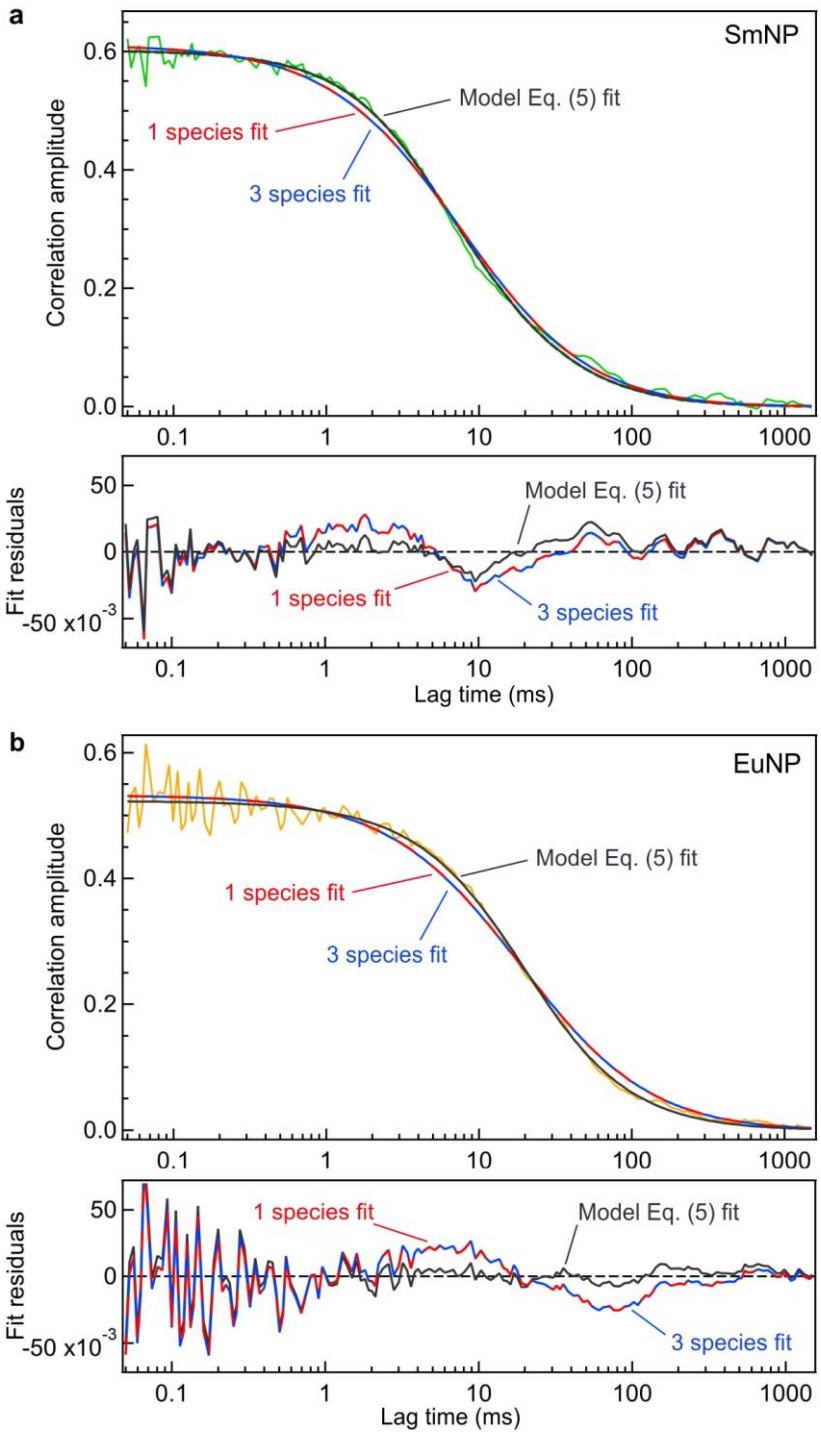

Figure S3. FCS correlation data for SmNPs (a) and EuNPs (b) together with the numerical fits and the fit residuals (lower graph). The fit using a single species (red trace) nearly perfectly overlaps with the fit using 3 species (blue trace). For the 3 species model, we set the relative diffusion times to follow the size histogram derived in Fig. 1, with diffusion times 0.75×, 1× and 1.25× the average diffusion time obtained from the single species fit. This led to no improvement in the fit residuals. Fitting with a 3 species model where all fit parameters are free led to an identical result as the 1 and 3 species fits shown here. The laser power was 20 µW for SmNP and 5 µW for EuNP.

S4. SmNP correlation data in viscous media

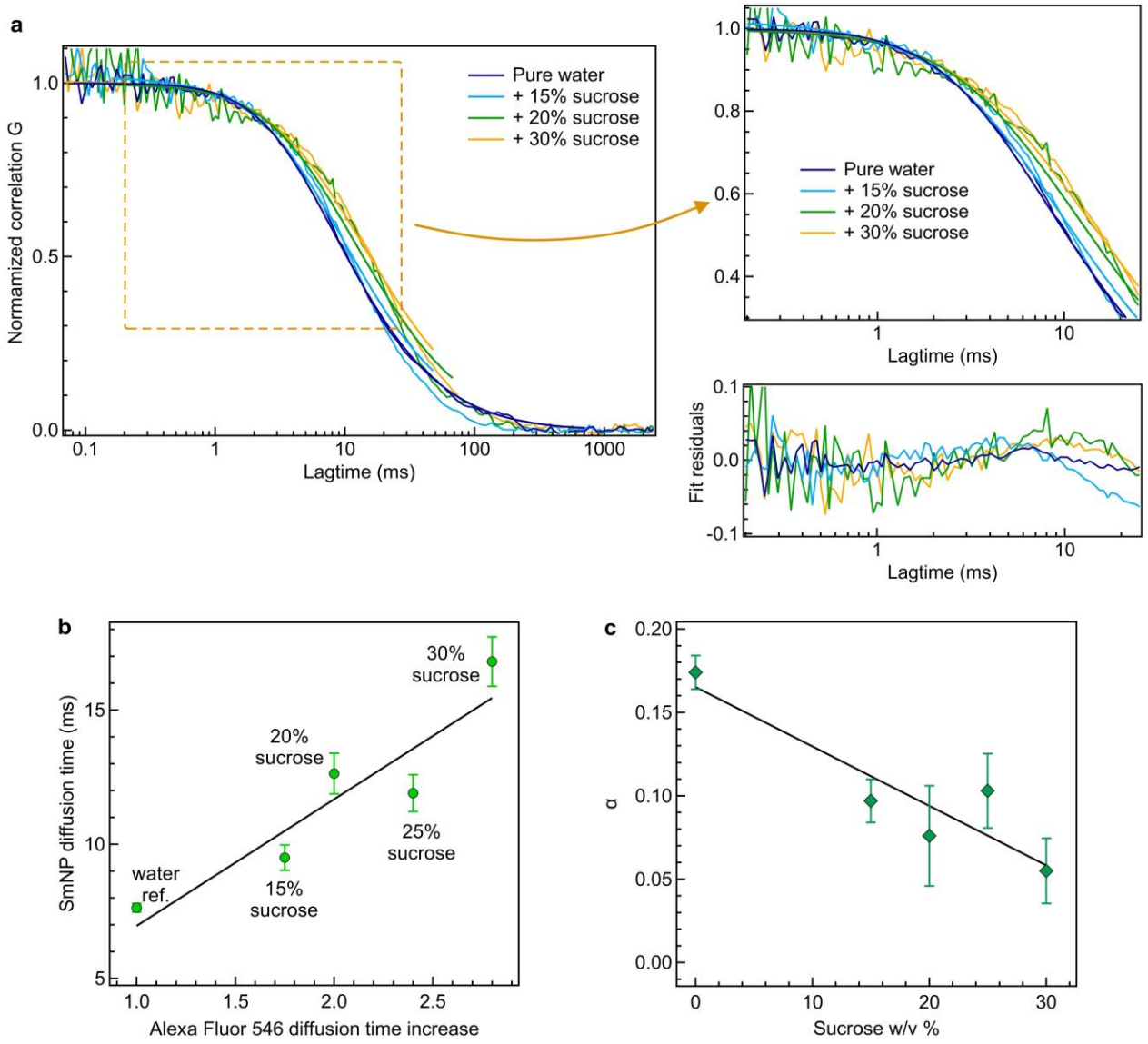

Figure S4. (a) FCS correlation data (thin lines) for SmNP in solutions containing different amounts of sucrose (in weight/volume) to increase the dynamic viscosity. The experimental conditions are similar to Fig. 3c, S2 and S3, with the excitation power being set to 20 µW. The thick color lines represent numerical fits using Eq. (5), where τ_A is set to correspond to the SmNP lifetime. (b) SmNP diffusion time τ_D for different sucrose concentrations. The influence of sucrose on the increase in the apparent FCS diffusion time was calibrated using standard FCS performed on Alexa Fluor 546 at 10 nM final concentration with the same microscope. We note a linear correlation (Pearson's correlation coefficient 92.5%) between the increase in the SmNP diffusion time τ_D and the increase in the diffusion time noted for Alexa Fluor 546. (c) Correction amplitude α using the model in Eq. (5) for different sucrose concentrations. The amplitude decreases with higher amounts of sucrose (Pearson's correlation coefficient -91.3%) but still remains clearly positive. These findings further substantiate the validity of our approach.

S5. Evolution of SmNP brightness as a function of laser power

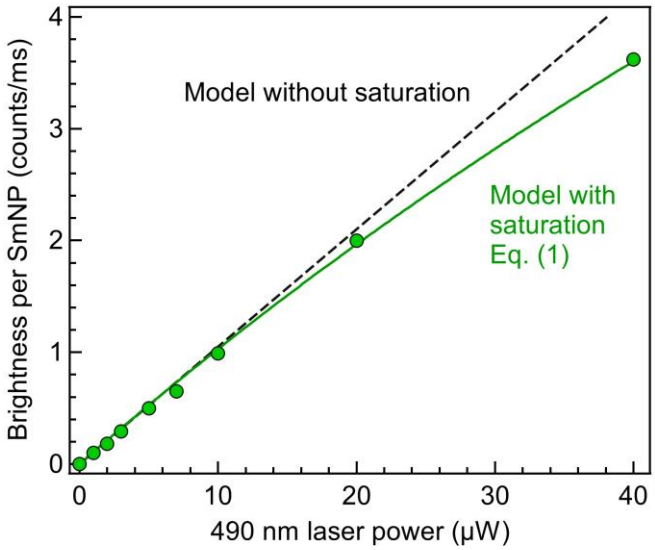

Figure S5. Evolution of the brightness per nanoparticle CRP as a function of the 490 nm laser power. The data is similar to Fig. 3d but on a broader power range, limited by the maximum laser power of our instrument at this illumination wavelength. Filled markers are experimental data points. The dashed line is a linear fit to the data, while the green line takes into account the saturation evolution based on Eq. (1). Using this data, we can estimate a saturation power around 200 µW for SmNPs.

S6. Transmission electron microscope and SEM images of SmNPs and EuNPs

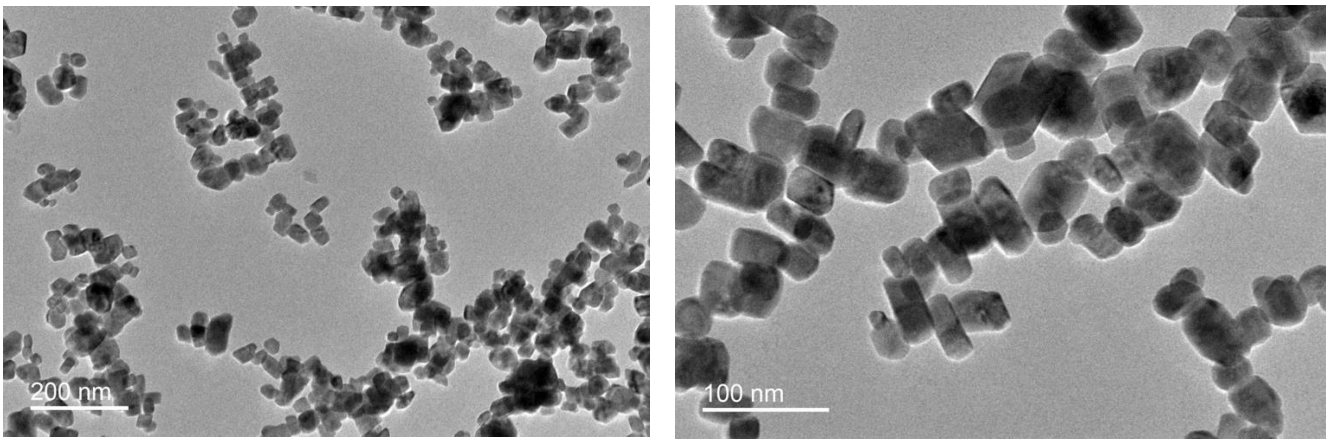

Figure S6. TEM images of SmNPs (La0.14Tb0.85Sm0.1F3). TEM revealed the presence of nanoparticles with an average diameter of 56 ± 15 nm, with a clearly elongated structure for the smallest particles. Transmission Electron Microscopy (TEM) was performed with a JEOL 2100F electron microscope operating at 200kV equipped with a GATAN GIF 200 electron imaging filter.

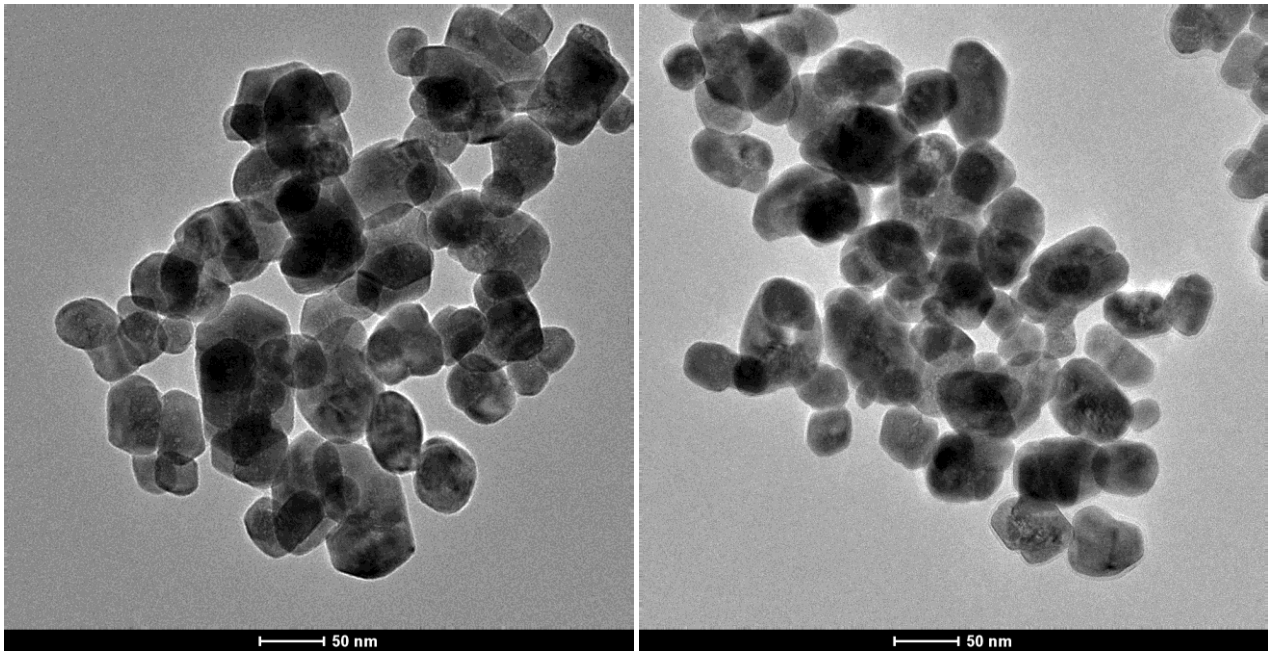

Figure S7. TEM images of EuNPs

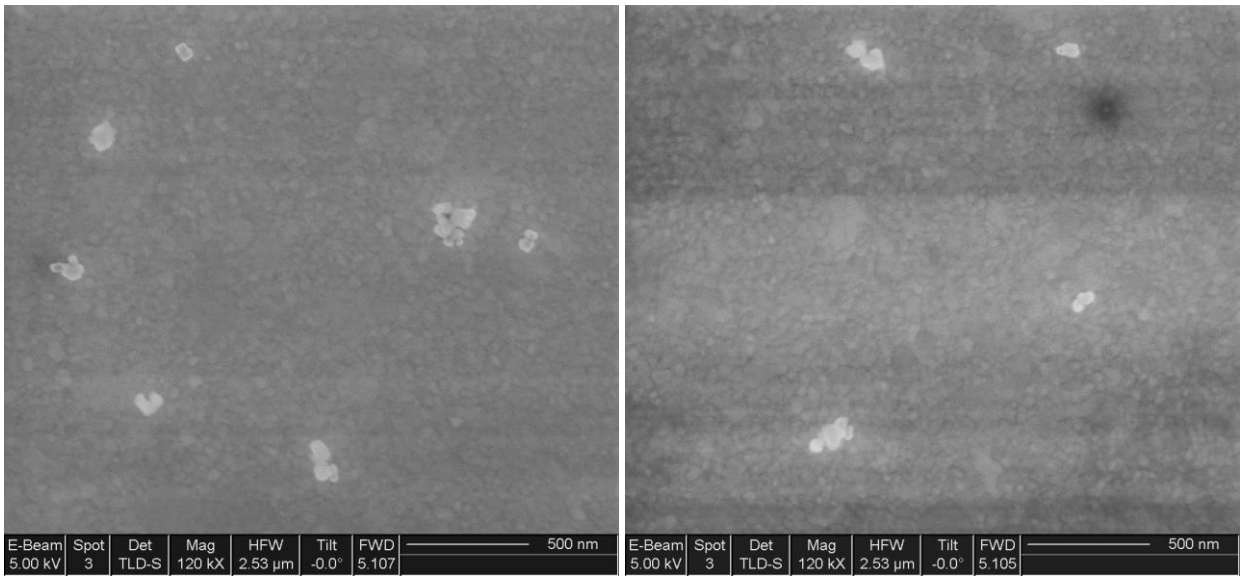

Figure S8. SEM images of SmNPs

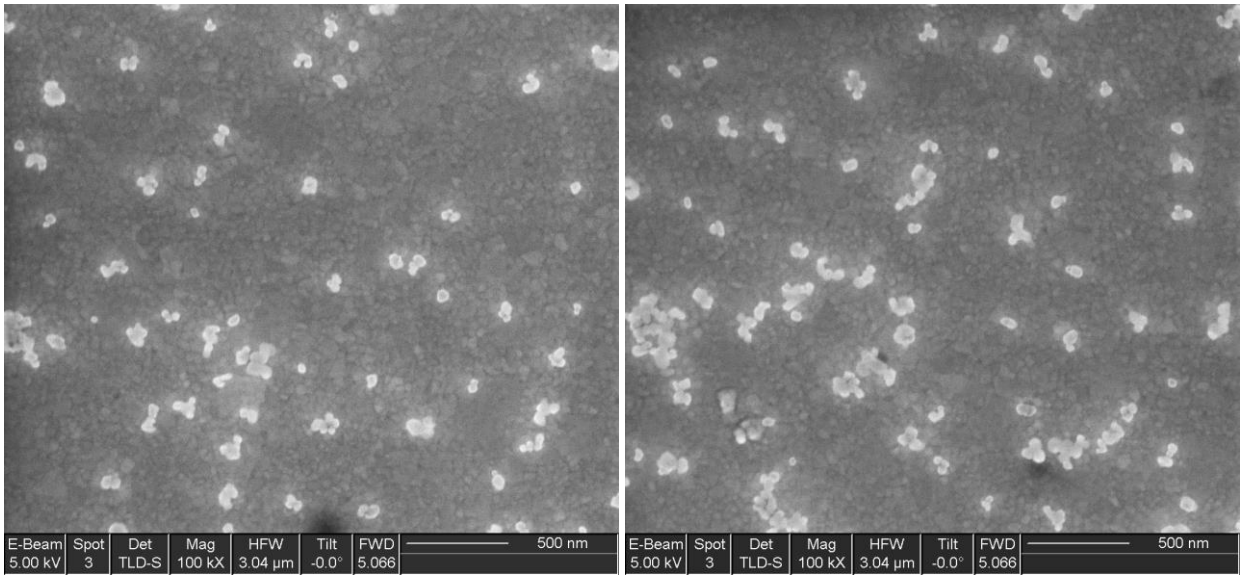

Figure S9. SEM images of EuNPs

S7. Detailed analysis of the nanoparticle

Type	*DLS (nm)*	*TEM (nm)*	*ICPAES results (mg/kg)*		
			La	*Sm*	*Tb*
Nps Tb/Sm/La 85%/1%/14%	*78*	*56*	*490*	*35*	*3116*
Nps Tb/Eu/La 85%/1%/14%	*83*	*64*	*540*	*49.3*	*4327*

Table S1. Inductively Coupled Plasma Atomic Emission Spectroscopy (ICP-AES) analysis of samples in water were performed with a Varian 720 spectrometer equipped with a quartz Meinhard nebulizer and a cyclone spray chamber. Anne Boos and Pascale Ronot are gratefully acknowledged for performing the ICP/AES analysis through the service of the inorganic analysis platform (PAI) at ECPM.

Reference: J. Goetz, A. Nonat, A. Diallo, M. Sy, I. Sera, A. Lecointre, C. Lefevre, C. F. Chan, K.-L. Wong, L. J. Charbonnière, *ChemPlusChem* **2016**, *81*, 526.